# Aging Investigation on 2024/Sic Composite and 2024 Alloy

**C. Badini, F. Marino and E. Verné - Dipartimento di Scienza dei Materiali e Ingegneria Chimica, Politecnico di Torino, (ITALY).**
**X.B. Guo* - Jinzhou Institute of Technology, Jinzhou (P.R. China).**

* Now at the Politecnico di Torino (I).

**Abstract**

*This paper is devoted to the study of natural and artificial aging of a 2024 aluminum alloy reinforced by 25% vol. SiC whiskers compared with a 2024 aluminum alloy, using differential scanning calorimetry and hardness measurements. All the samples were solutionized at 529°C and naturally aged up to 60 days or artificially aged at 190°C up to 200 hours. For what concerns natural aging the mechanism is the same for the two materials resulting only in the formation of G.P. zones. The natural aging rates are similar , therefore the composite and the matrix attain the maximum hardness after 3 days of aging. From this evidence it can be inferred that a spinodal decomposition takes place instead of a nucleation phenomenon in the formation of G.P. zones. Artificial aging leads to a microstructure constituted by ϑ"+ϑ'+S' metastable phases, which results in the best aging response for both materials. In these conditions the composite ages more quickly with respect to the unreinforced alloy, in fact the aging at 190°C involves nucleation phenomena and the different dislocation density in the two materials are now effective. If the same thermal cycle of the 2024 A.A. is used for 2024/SiC an overaging condition is attained.*

**Riassunto**

Questa pubblicazione é rivolta allo studio dell'invecchiamento naturale e artificiale di un composito con matrice in lega di alluminio 2024 e rinforzata con il 25% vol. di whiskers di SiC, raffrontato con una lega 2024. Le tecniche sperimentali utilizzate a tale scopo sono state la calorimetria differenziale a scansione e le misure durometriche.
Tutti i campioni sono stati solubilizzati a 529°C, quindi alcuni invecchiati naturalmente fino a 60 giorni; altri artificialmente a 190°C fino a 200h.
Il meccanismo che conduce all'invecchiamento naturale é identico per i due materiali e porta alla formazione delle zone GP; le velocità d'invecchiamento sono simili: matrice e composito raggiungono il massimo di durezza dopo tre giorni di trattamento. Questo dato induce ad ipotizzare che la formazione delle zone GP avvenga attraverso un meccanismo di decomposizione spinoidale e non di nucleazione e crescita.
L'invecchiamento artificiale conduce ad una microstruttura costituita dalle fasi ϑ"+ϑ'+S' la cui presenza garantisce le proprietà meccaniche ottimali per entrambi i materiali.
Durante l'invecchiamento artificiale il composito invecchia più rapidamente che la matrice, e questo perché il trattamento a 190°C attiva una trasformazione di nucleazione eterogenea e crescita e quindi la maggior concentrazione di dislocazioni, presente nel composito, fa sentire il suo effetto sulla cinetica di trasformazione.
Se per il composito viene utilizzato lo stesso ciclo di trattamento termico della corrispondente lega di alluminio, in termini di matrice, si raggiungono le condizioni, non desiderabili, di super invecchiamento.

## Introduction

In the last thirty years, many developments have occurred in the field of metal matrix composites (MMCs); the majority of the research work on this topic has dealt with the processing of these materials. The last step of MMCs fabrication generally involves a thermal treatment suitable to enhance the mechanical properties of their metal matrix. These thermal treatments are the same normally used in order to strengthen the unreinforced light alloys, however, in the case of composites, the treatments should be designed taking into account the peculiar characteristics of these materials. In this paper the aging behaviour of an Al-Cu-Mg/SiC composite is compared with that of the corresponding unreinforced alloy. The precipitation sequence in Al-Cu alloys was extensively investigated [1-6]. The aging path of Al-Cu supersaturated solid solutions, obtained by solution and quenching, involves the formation of Guinier Preston (G.P.) zones, tetragonal ϑ", tetra-

gonal semicoherent ϑ' and stable ϑ ($Al_2Cu$). It was extensively debated whether ϑ" has to be regarded as a particular kind of G.P. zones or whether it is a distinct phase. There are several arguments which support the second hypothesis: ϑ" shows a distinct ordered crystal structure and a solvus curve different from those of G.P. zones. Furthermore, there is no complete agreement in literature about the question whether ϑ" is fully coherent with the matrix or not [1-4], even though complete coherence seems more probable.In Al-Cu-Mg alloys another aging sequence was also observed; according to this second sequence the strengthening is achieved by the consecutive formation of the following phases: G.P. zones (containing Al, Cu and Mg), semicoherent S' (orthorhombic) and stable S ($Al_2CuMg$) [2,4]. These two precipitation sequences can occur contemporaneously in Al-Cu-Mg alloys giving rise to the formation of both $Al_2Cu$ and $Al_2CuMg$ precipitates with a percentage depending on the Cu/Mg ratio

Thermal analysis was frequently used in order to characterize the microstructure of Al-Cu and Al-Cu-Mg alloys and to investigate the precipitation mechanism [7-11]. The thermograms reported in literature on this topic showed some appreciable variances and gave rise to different interpretations [7-11]. This topic was discussed in a previous paper [12] with the purpose of assigning each thermal effect, shown in the Differential Scanning Calorimetry (DSC) curves, to a specific step of the precipitation sequence. In this work DSC and hardness measurements are used to compare the aging response of an Al-Cu-Mg alloy to that of an Al-Cu-Mg/SiC composite. As the aging process causes only a change in the matrix microstructure, its mechanism is not affected by the ceramic reinforcement. However, the presence of ceramic reinforcement has been shown to accelerate the artificial aging process of MMCs with respect to the unreinforced materials [13-19]. The accelerated aging for reinforced alloys has been attributed to the presence of a high density of dislocations, resulting from the difference in the thermal expansion coefficient between the ceramic and the metal matrix, and, consequently, to the presence of several nucleation sites causing the heterogeneous precipitation of the hardening phases [13-19]. On the contrary, this influence of ceramic reinforcement on aging kinetics was not observed in the case of Al-Cu and Al-Cu-Mg metal matrix composites. In fact, according to Kim et al. [10] the SiC reinforcement delays (slows down) the artificial aging of an Al-4%Cu alloy. According to Papazian [8] the aging kinetic of 2124/SiC composite is not appreciably different from that of the corresponding Al-Cu-Mg unreinforced alloy.

## Experimental part

The behaviour of an Al-Cu-Mg/SiCw composite was compared with that of 2024 (Al-Cu-Mg) unreinforced alloy. The chemical compositions of both aluminum based alloy and the composite metal matrix are reported in Table 1. Bars of composite (25% vol. SiC whiskers, 28 mm in diameter) were produced by BP Metal Composites by powder metallurgy and hot extrusion. The 2024 reference alloy was fabricated by casting and hot extrusion. Discs about 10 mm thick were prepared by cutting the extruded bars transversally with respect to their axes. These samples were metallographically polished, submitted to thermal treatment and indented in order to measure the material hardness corresponding to various aging times. Brinell hardness measurements were carried out with a load of 625 MPa using a sphere (2.5 mm in diameter) as indenter. At least 12 measurements were averaged for each aging time. Small bars (5 mm in diameter) were machined from the extruded bars (in the longitudinal direction) and thin slices (about 50-70 mg in weight) were cut from these smaller bars; these specimens were used for thermal analysis. All the samples were solutionized at 529±5 °C (2.5 hours) in a salt bath, quenched in a brine bath and aged in different conditions. Natural aging at room temperature and artificial aging (performed in an oil bath at 190±3 °C) were carried out up to two months and 200 hours respectively. After different aging periods, the samples were stored in liquid nitrogen before being submitted to thermal analysis or hardness measurements. Differential Scanning Calorimetry (DSC) was performed under argon atmosphere using a DSC7 Perkin Elmer equipment. The method used in this analysis was detailed elsewhere [18,20]. Different scanning rates (from 2 to 50 °C/min) were used in this study.

**TABLE 1 - Chemical composition of 2024 alloy and 2024/SiC metal matrix.**

| Material | Chemical composition wt %. | | | | | |
|---|---|---|---|---|---|---|
| | Cu | Mg | Fe | Ni | Mn | Al |
| Composite matrix | 3,43 | 0,96 | 0,24 | 0,01 | 0,79 | balance |
| 2024 alloy | 4,25 | 1,30 | 0,22 | 0,01 | 0,48 | balance |

## Results and discussion

### Natural aging

Fig.1 shows the DSC patterns of 2024 samples thermally treated under different conditions: after solution treatment and quenching (curve a); after solution, quenching and aging at room temperature for 12, 24, 48, 72 and 168 hours (curves b, c, d, e and f respectively). Temperatures and enthalpies related to thermal effects in some of these DSC curves are reported in Table 2. As discussed in a previous paper [12], all the transformations that may be involved in the aging phenomena are appreciable in the DSC trace of a solutionized and quenched sample. The attribution of thermal effects to each step of the aging path was done in [12] by means of calorimetric experiments and using the metastable solvus curves reported in the literature [1] for GP zones, $\vartheta''$ tetragonal phase and $\vartheta'$ semicoherent tetragonal (showing different lattice parameters with respect to $\vartheta''$ ) . In addition, the presence of magnesium in the 2024 alloy causes the formation of specific G.P. zones and, subsequently, the precipitation of semicoherent metastable S' ($Al_2CuMg$). This last phenomenon was attributed to an exothermal effect in DSC thermograms by comparing these thermograms with the DSC curve of a solutionized 2618 alloy, which ages through the formation of S' only.

In the DSC trace "a" of fig.1 (pertaining to a solutionized and quenched specimen) the following effects can be appreciated with the increase in temperature :
- a broad exothermal peak (A) due to G. P. zones formation;
- a structured endothermic effect (B, B') related to G.P. zone dissolution (different kind of zones form in this alloy [4-6, 11] );
- two strong exothermal peaks (C,D), more or less overlapped depending on the scanning rate and on the chemical composition of the alloy, which were attributed to $\vartheta''$ and $\vartheta'$+S' formation.

During the natural aging of 2024 the DSC trace progressively changes due to the formation of G.P. zones. This phenomenon results in the progressive decrease in intensity of the first exothermal peak which disappears after 24 hours of aging (Table 2).The two peaks (C,D) become more strongly overlapped with aging time. These exothermal peaks are distinguishable up to 72 hours of aging. After this time a very large effect, showing a plateau instead of two maxima, appears in the thermogram (curve f of Fig.1). On the other hand , the enthalpy related to metastable $\vartheta''$, $\vartheta'$ and S' precipitation does not change appreciably with the aging time (Table 2), showing that natural aging only involves the formation of G.P. zones.

**TABLE 2 - Peak temperatures (°C) and entalphy values (J/g) from thermograms (scanning rate 20 K/min) of solutionized and naturally aged 2024 and 2024/SiC composite (sol. = solution treated).**

| Sample | Peak | | | | | | |
|---|---|---|---|---|---|---|---|
| | A (G.P. form.) | | B+B' (G.P. diss.) | | C+D (ϑ"+ϑ'+S') | | |
| | $\Delta H$ | $T_A$ | $\Delta H_{tot.}$ | $T_B$ | $\Delta H_{tot.}$ | $T_C$ | $T_D$ |
| 2024 sol. | 7 | 92 | 5 | 238 | 33 | 286 | 307 |
| 2024/SiC sol. | 3 | 91 | 5 | 230 | 19 | 278 | |
| 2024 12h | 1 | - | 5 | 236 | 28 | 284 | 304 |
| 2024/SiC 12h | - | - | 4 | 229 | 19 | 278 | |
| 2024 24h | 0,5 | - | 4 | 237 | 29 | 285 | 306 |
| 2024/SiC 24h | - | - | 5 | 228 | 19 | 279 | |
| 2024 72h | - | - | 4 | 241 | 28 | 284 | 305 |
| 2024/SiC 72h | - | - | 2 | 230 | 20 | 279 | |

Natural aging of 2024/SiC composite results in a modification of DSC traces similar to that observed for the aging of the unreinforced alloy. In this case the zone formation is already complete after 12 hours of aging (fig.2, Table 2). It is worth noting that the exothermal peaks for transition phase precipitation (C,D) are not distinguishable in the traces of 2024/SiC obtained with a scanning rate of 20°C/min because the second peak shows an intensity much lower than the former. This is due to the different amount of $Al_2Cu$ and $Al_2CuMg$ precipitated in the composite matrix with the respect to the unreinforced alloy, which is caused by a different Cu/Mg ratio in the two materials.

As reported elsewere [12] the peaks C and D become distinguishable with scanning rates of 10 and 5°C/min. The Brinell hardness evolution against aging time (fig.3) is very similar for the two materials which achieve the maximum strength after aging periods longer than 3 days. As the formation of G.P. zones is complete after 24 or 12 hours in 2024 and 2024/SiC respectively, and as the maximum hardness of the materials is not achieved at these aging times, probably the better aging response is reached only with a suitable zone growth. As fig. 1 and 2 show, in the complex endothermal area related to G.P. zone dissolution two sharp distinct effects are better appreciable after 3 days of aging, corresponding to the achieving of the maximum hardness. According to literature [1] copper is not randomly distributed in the Al-Cu supersaturated solid solution, in which small copper rich regions prefigure the structure of G.P. zones. It was suggested that zones form continuously from this modulated microstructure by spinodal mechanism. As a consequence, the different dislocation concentration in unreinforced alloy and composite matrix does not affect the kinetic for the early stages of zone formation. On the contrary, dislocations are known to increase the nucleation rate, because solute atoms preferentially diffuse towards dislocations, where the elastic field due to solute atoms can be balanced by the elastic field of a dislocation. After the formation of G.P. zones they should grow by diffusion of solute atoms, which is basically affected by the vacancy concentration generated by solution and quenching processes. This mechanism for zone formation justifies the similar aging kinetics of alloy and composite but not the differences in DSC traces corresponding to the beginning of aging, i.e. the disappearance of peak A after different aging times for the two materials.

## Artificial aging

DSC thermograms of solutionized and artificially aged samples (corresponding to different aging periods) of 2024 and 2024/SiC composite are compared in fig. 4 and 5 respectively. Aging at 190°C causes the immediate disappearence of the exothermal peak for zone formation and a decrease in the peak intensities for both zone dissolution and metastable precipitate formation (Table 3 ). In addition, the peak for G.P. zone dissolution shifts towards higher temperatures as the aging process advances and the subsequent exothermal effects (peaks C and D) become more weak (Table 3 ). Figure 4 shows that in the DSC trace of 2024 sample the two exothermal peaks for precipitation of transition phases are still distinguishable after two hours of aging as well as the endothermic phenomenon B. Hence, it can be supposed that the early stage of artificial aging involves the formation of G.P. zones. On the contrary, DSC analysis does not allow us to state whether G.P. zones are still present in the microstructure of both 2024 and 2024/SiC composite after longer aging time, even though the endothermic effect B was also observed in the corresponding thermograms. Actually there is some disagreement in literature about the solvus curve of G.P. zones [1-3], which, for chemical compositions like that of our samples, lies near the temperature recommended by Metals Handbook [21] for artificial aging of 2024 alloy. However, as aging process has to be considered a continuous process and as $\vartheta$" and G.P. zones are so similar that in the past $\vartheta$" was regarded as a kind of zones,it is difficult to state how much G.P. zones, after a growth in size, differ from $\vartheta$". Probably the exothermal effect related to the formation of $\vartheta$" (peak C) should become weaker with the G.P. zone growth and modification. In fact peak C disappears and the endothermic effect B greatly shifts towards high temperatures with the aging time. Hence, the endothermic peak (B) in the thermograms of artificially aged samples should be attributed to the dissolution of more or less modified zones. The subsequent exothermal effect (D) has to be related to the formation of semicoherent phases ($\vartheta$'and S'). Artificial aging also involves the precipitation of semicoherent phases, resulting in the progressive decrease of this exothermal peak (D). The DSC trace modification for composite (fig. 5) is similar to that observed for 2024, although the overlap of exothermal effects (C and D) does not permit to appreciate the disappearance of peak C before the intensity decrease of peak D. On the other hand, in the composite DSC thermograms, the precipitation of $\vartheta$" (disappearance of effect C) could cause the observed shift of the maximum temperature of overlapped C+D phenomenon (Table 3). The aging rate is very different for the two materials, in fact, the precipitation of the semicoherent phases is almost complete after 28 h in the case of 2024 alloy while only 8 h of aging are sufficient to accomplish the same phenomenon in the composite. In addition, all the transformations involved in the aging sequence occur, during a DSC scan of solutionized samples, at lower temperature in the case of the composite with respect to aluminum alloy (Table 3). The different aging behaviour is also put in evidence by the hardness evolution during aging. Fig. 6 shows that the composite reaches the maximum hardness for times between 2 and 10 hours, contrary to 2024 alloy which presents maximum hardness between 10 and 30 hours of aging. The accelerated aging of composite can be explained with the higher dislocation concentration. To this purpose it is worthy of note that Al-Cu G.P. zones are known to form above 130°C with a mechanism different from that suggested for low temperature; when aging above 130°C the spinodal decomposition is suppressed and zones nucleate from the solid solution [1]. Furthermore, the hardness increase caused by aging is about 250 MPa (25 $kg/mm^2$) and 420 MPa.

The poor aging response of the composite can be explained taking into account the SiC presence and the lower content of alloying elements in the composite matrix. Furthermore, in the case of the composite, the transition phases nucleate heterogeneously, because this phenomenon occurs preferentially in the part of the matrix close to ceramic reinforcement, where there is a higher dislocation density. Figure 7 shows that the distribution of small size precipitates is homogeneous inside a sample of unreinforced 2024 aged for 8 hours. Figure 8 shows the microstructure of 2024/SiC composite after 2 hours of aging. In fig. 8a the distribution of SiC whiskers is depicted; fig. 8b highlights the hardening precipitates after chemical etching. In the case of the composite the precipitation chiefly happens heterogeneously near the particles of ceramic reinforcement. In the part of the matrix free of SiC only few precipitate crystals are present. As the maximum hardness is

associated with the precipitate attaining a critical size and distribution when the precipitation is not homogeneous, the precipitate is less effective in retaining dislocation motion.

**TABLE 3 - Peak temperatures (°C) and enthalpy values (J/g) from thermograms (scanning rate 20 K/min) of solutionized and artificially aged (at 190 °C) 2024 and 2024/SiC composite (sol. = solution created; sh.=shoulder).**

| Sample | Peak | | | | | | |
|---|---|---|---|---|---|---|---|
| | A (G.P. form.) | | B+B' (G.P. diss.) | | C+D (ϑ"+ϑ'+S') | | |
| | $\Delta H$ | $T_A$ | $\Delta H_{tot.}$ | $T_B$ | $\Delta H_{tot.}$ | $T_C$ | $T_D$ |
| 2024 sol. | 7 | 92 | 5 | 238 | 33 | 286 | 307 |
| 2024/SiC sol. | 3 | 91 | 5 | 230 | 19 | 278 | |
| 2024 2h | - | - | 5 | 243 | 32 | sh. | 307 |
| 2024/SiC 2h | - | - | 3 | 236 | 14 | 281 | |
| 2024 8h | - | - | 4 | 249 | 18 | - | 307 |
| 2024/SiC 8h | - | - | 0,5 | 249 | 1 | 290 | |
| 2024 12h | - | - | 4 | 253 | 16 | - | 306 |
| 2024/SiC 12h | - | - | - | - | - | - | |
| 2024 16h | - | - | 3 | 257 | 9 | - | 309 |
| 2024 20h | - | - | 2 | 260 | 6 | - | 312 |
| 2024 28h | - | - | 1 | 261 | 3,5 | - | 310 |

The comparison between the shape of DSC traces of differently aged samples and the hardness curves allows us to recognize what is the sample microstructure which gives the best mechanical properties. When a sample is heated at 190°C G.P. zones immediately form. After this step the zones grow and transform progressively into ϑ, ϑ' and S' transition phases.This last phenomenon causes a decrease in the amount of residual G.P. zones , as showed by the decrease in the enthalpy involved in their dissolution (peak B in DSC traces, Table 3). This peak enthalpy is related to the amount of more or less modified G.P. zones present in the samples. The enthalpy of exothermal peaks (C+D), measured in the DSC thermogram of solution treated specimens, can be regarded as an evaluation of the whole energy involved in the complete formation of transition phases. The partial formation of these precipitates during aging results in the decrease of this enthalpy value in DSC curves. The difference in C+D peak enthalpy between solution treated and solution treated and aged samples can be used to approximatively estimate how much the precipitation of intermediate phases proceeds during aging. The enthalpy values related to the amount of both zones and transition phases present in aged samples are plotted in figure 9 against the aging time. In the case of the composite the enthalpy values are referred to one gram of metal matrix. The best aging response is achieved when all these kinds of precipitates are present in the aluminium alloy microstructure. The over aging, that is the loss in hardness, starts with the complete precipitation of ϑ' and S'.

## Conclusions

### Natural aging

DSC analysis shows that the mechanism for natural aging is the same for 2024 alloy and 2024/SiC composite: the material strengthening is due to the formation and growth of Guinier Preston zones.
DSC traces aging results in the progressive disappearance of the exothermal peak related to G.P. zone formation.
Moreover the aging rates of 2024 and the composite are similar at room temperature. In fact, at low temperatures the zone formation occurs by a spinodal decomposition; hence the rate of this process is not affected by the higher dislocation density in the composite matrix.
The two materials both achieve the maximum hardness after 3 days of aging.

### Artificial aging

Artificial aging of 2024 and 2024/SiC involves the formation firstly of G.P. zones and subsequently of the intermediate phase $\vartheta$' and S'. These phenomena result in the following DSC curve modifications:
- a progressive disappearance of the endothermic peak (attributed to the dissolution of G.P. zones) and a shift of this peak towards higher temperatures;
- a progressive decrease of exothermal effects related to the formation of metastable $\vartheta$' and S' phases.

The contemporaneous presence of these three phases results in the best aging response for both materials.
The composite ages more quickly with respect to the unreiforced alloy because in the first case (material) a higher dislocation concentration at the reinforcement/matrix interfaces accelerates the heterogeneous precipitation of the hardening phases.
The maximum hardness is reached more rapidly for the composite whith respect to the 2024 alloy.Thus the thermal treatment of the composite under the same conditions usually adopted for 2024 can cause an overaging.

## References


[1] J.L. Murray, *Int. Metals Reviews* , 30 (1985) 211.
[2] C.R. Brooks, *Heat treatment, structure and properties of non-ferrous alloys,* American Society for Metals, Metals Park, Ohio, USA, (1982).
[3] D.A. Porter, K.E. Easterling, *Phase transformations in metals and alloys*, Van NostrandReinhold, U.K., (1987).
[4] M. Conserva, E. Di Russo, P. Fiorini, *Alluminio e Nuova Metallurgia*, XIX (1970) 515.
[5] X. Auvray, P. Georgopoulos and J.B. Cohen, *Acta Metall.*, 29 (1981) 1061.
[6] K. Osamura, Y. Murakami, T. Sato, T. Takahashi, T. Abe and K. Hirano, *Acta Metall.*, 31 (1983) 1669.
[7] S. Abis and G. Riontino, Z. Metallk.de , 79 (1988) 202.
[8] J.M. Papazian, Metall. Trans., 19 A (1988) 2945.
[9] J.M. Papazian and P.N. Adler, Metall. Trans., 21A (1990) 401.
[10] T.S. Kim, T.H. Kim, K.H. Oh, H.I. Lee, J. Mater. Sci., 27 (1992) 2599.
[11] A.K. Jena, A.K. Gupta and M.C. Chaturvedi, *Acta Metall*, 37 (1989) 885.
[12] C. Badini, F. Marino, E. Verné. Mater. Sci. Eng., in print.
[13] T.G. Nieh and R.F. Karlak, *Scripta Metall.*, 18 (1984) 25.

[14] T. Christman and S. Suresh, *Acta Metall.*, 36 (1988) 1691.
[15] I. Dutta, D.L. Bourell, D. Latimer, J. Compos. Materials, 22 (1988) 829.
[16] S. Suresh, T. Christman and Y. Sugimura, *Scripta Metall.*, 23 (1989) 1599.
[17] I. Dutta and D.L. Bourell, *Acta Metall.* Mater., 38 (1990) 2041.
[18] C. Badini, F. Marino, A. Tomasi, Mater. Chem. Phys., 25 ( 1990 ) 57 .
[19] S.M. Seyed Reihami, D. Dafir and P. Merle, *Scripta Metall. Mater.*, 28 (1993) 639.
[20] Appendino, C. Badini, F. Marino, A. Tomasi, Mater. Sci. Eng., 135A (1991) 275.
[21] Metals Handbook, American Society for Metals, 8 th edn., Metals Park, Ohio, USA, Vol.8 (1973) pp. 72-75.

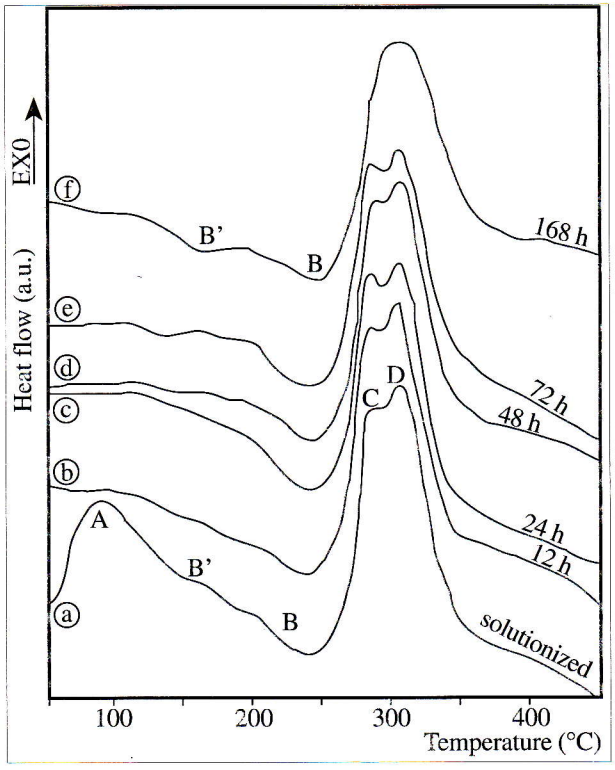


Fig. 1
DSC curves of 2024 unreinforced alloy: a= solution treated and quenched; b, c, d, e, f = solution treated, quenched and naturally aged for 12, 24, 48, 72 and 168 hours respectively. Scanning rate: 20 K/min

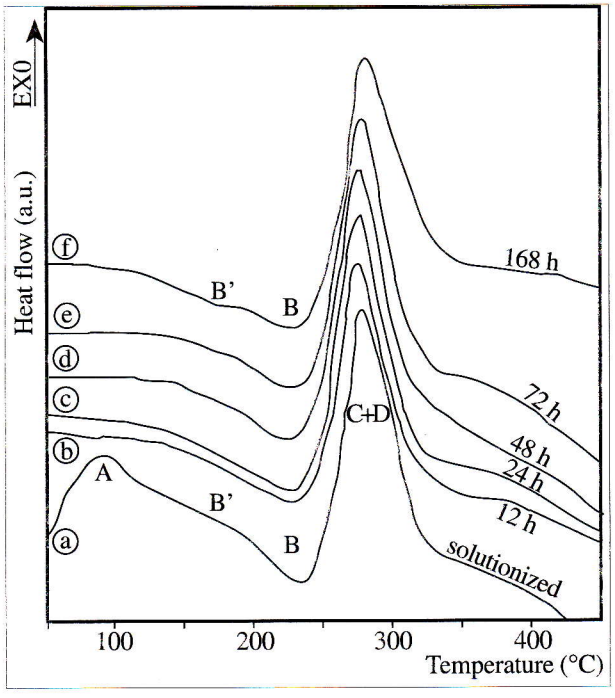


Fig. 2
DSC curves of 2024/SiC composite : a= solution treated and quenched; b, c, d, e, f = solution treated, quenched and naturally aged for 12, 24, 48, 72 and 168 hours respectively. Scanning rate: 20 K/min

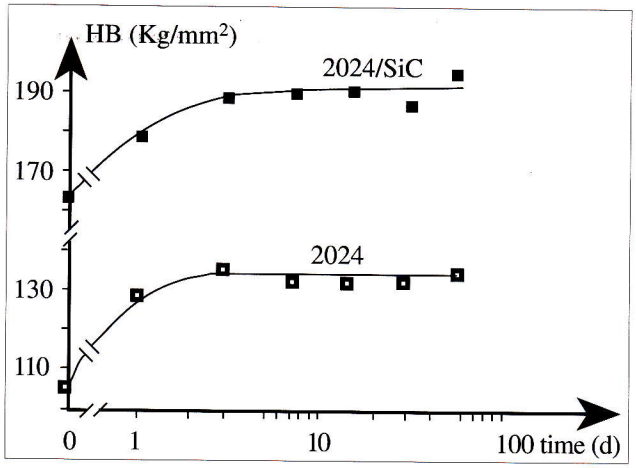


Fig. 3
Brinell hardness against aging time at room temperature for 2024 alloy and 2024/SiC composite.

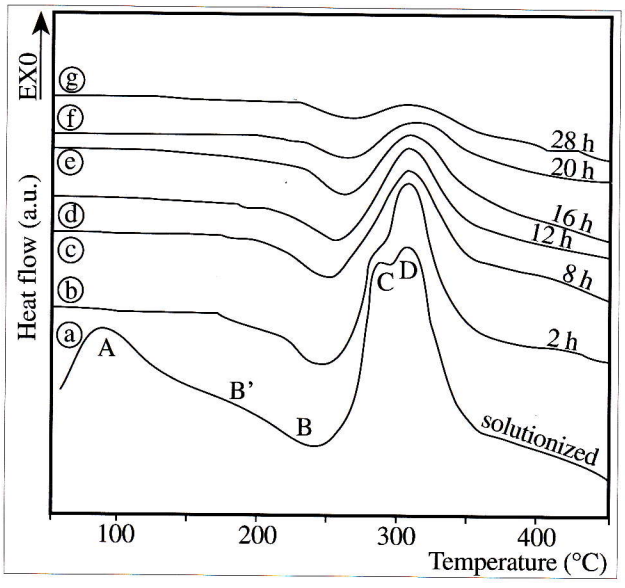


Fig. 4
DSC curves of 2024 alloy: a= solution treated and quenched; b,c,d,e,f,g = solution treated, quenched and artificially aged for 2,8,12,16,20,28 hours at 190°C. Scanning rate 20 K/min

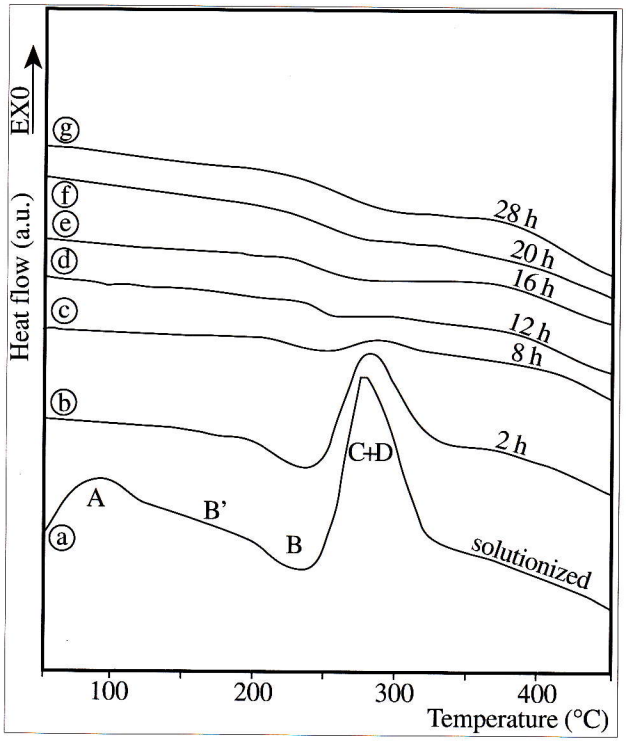


Fig. 5
DSC curves of 2024/SiC composite: a= solution treated and quenched; b,c,d,e,f,g = solution treated, quenched and artificially aged for 2,8,12,16,20,28 hours at 190°C. Scanning rate: 20 K/min

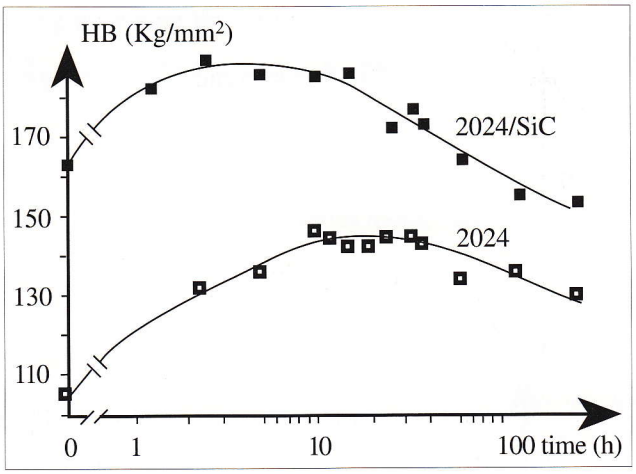


Fig. 6
Brinell hardness against time for 2024 alloy and 2024/SiC composite aged at 190°C.

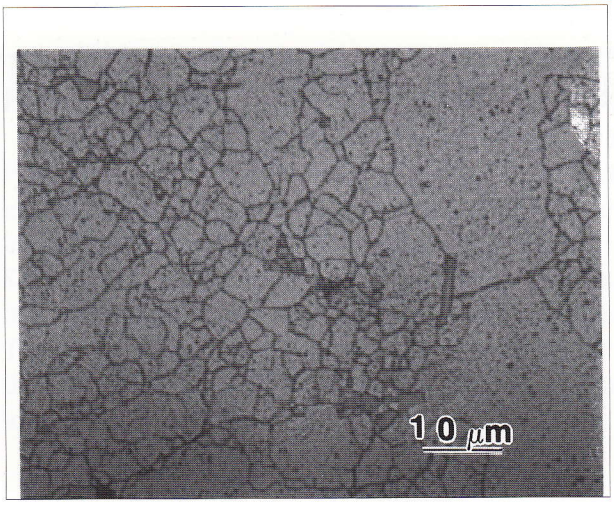


Fig. 7
Microstructure of 2024 alloy artificially aged until the maximum hardness (8 h. at 190°C); etching $HNO_3$ 25%.

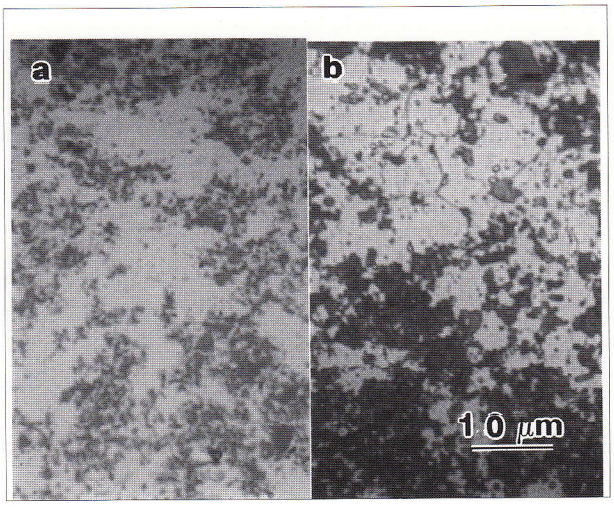


Fig. 8
Microstructure of 2024/SiC composite artificially aged until the maximum hardness (2 h. at 190°C); a= distribution of SiC reinforcement (no etching), b= distribution of reinforcement and hardening precipitates (etching $HNO_3$ 25%).

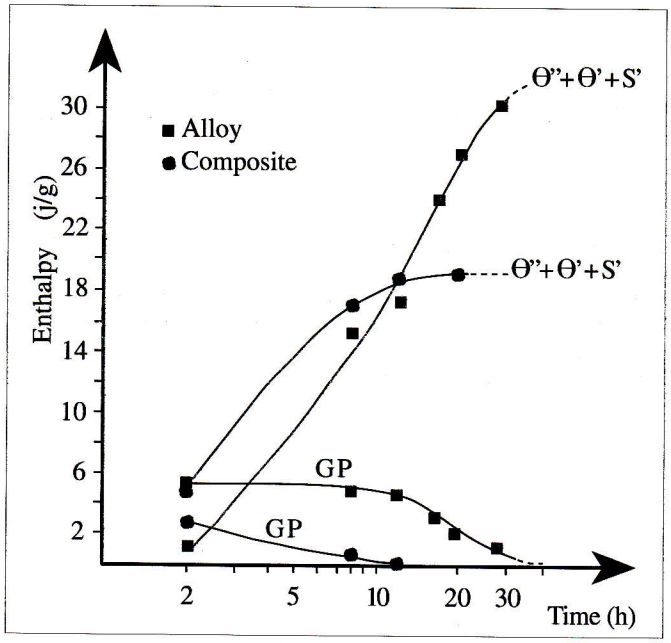


Fig. 9
Enthalpy values related to G.P. zones and intermediate phases present in the samples after different aging times.